

## Tunable Metastability of Surface Nanostructure Arrays

D. E. Jesson

*School of Physics and Materials Engineering, Monash University, Victoria 3800, Australia*

T. P. Munt

*Department of Physics, School of Engineering and Physical Sciences, Heriot-Watt University, Edinburgh EH14 4AS, United Kingdom*

V. A. Shchukin\* and D. Bimberg

*Institut für Festkörperphysik, Technische Universität Berlin, D-10623 Berlin, Germany*

(Received 10 November 2003; published 17 March 2004)

A Fokker-Planck equation is used to model the coarsening of surface nanostructure arrays. Metastable states are identified which are associated with a narrow size distribution and a coverage dependent mean island size. This is a general feature linked to nanostructures which, as a function of island size, are associated with a minimum in formation energy per atom and a positive chemical potential gradient. This has important implications for the self-organization of quantum dots.

DOI: 10.1103/PhysRevLett.92.115503

PACS numbers: 81.07.Ta, 68.35.Md, 68.65.-k, 81.16.-c

The spontaneous formation of nanoscale structures on surfaces using thin film deposition techniques, such as molecular beam epitaxy, offers an attractive route for the self-assembly of three-dimensional semiconductor islands or quantum dots [1–5]. These structures have important applications in the design of novel devices such as quantum dot lasers [6]. However, size uniformity is a critical issue for potential device applications which has led to significant efforts to understand the kinetic [7–20] and thermodynamic [21–27] factors governing the coarsening of quantum dot arrays.

In this Letter we consider the coarsening of surface nanostructures which, as function of island size, are associated with a minimum in the island formation energy per atom. In principle, these are particularly attractive candidates for attaining narrow size distributions because a thermodynamically favored size exists [21–24]. Such nanostructures include strained 2D islands [21,22] as well as 3D islands with strain renormalized surface energy [23,24]. The new feature identified in this work is the existence of dynamic metastable states which naturally arise as a competition between chemical potential driven drift and thermal diffusive broadening of the island size distribution. Most importantly, the size distribution function approaches a Gaussian form with a coverage dependent mean island size, allowing the fabrication of uniformly sized arrays with size selectivity.

To illustrate the concepts of tunable metastability, we focus on a mathematically tractable system consisting of 2D strained islands where it is generally accepted that a thermodynamically favored size exists [21,22]. We emphasize, however, that our qualitative conclusions regarding metastability are quite general and depend only on individual nanostructures possessing a minimum (i.e., a positive gradient) in chemical potential as a function of island size.

For a dilute array of islands, the energy of formation of a single island consisting of  $N$  atoms is given by

$$E(N) = -WN + C_1\sqrt{N} - C_2\sqrt{N}\ln(\sqrt{N}). \quad (1)$$

The first term is the binding energy between the adsorbate atoms, and the second term is the island edge energy due to broken chemical bonds. The third term is the elastic relaxation energy associated with the discontinuity of the surface stress tensor at the island boundaries which results in elastic relaxation for heteroepitaxial systems. The energy per atom,  $\varepsilon(N) = E(N)/N$ , is plotted in Fig. 1(a). It always has a minimum at the optimum size  $N_0 = \exp[2(C_1/C_2 + 1)]$  at which the energy per atom is lower than in a fully ripened island ( $N \rightarrow \infty$ ) by the quantity  $\varepsilon_0 = C_2N_0^{-1/2}$ . The chemical potential of the island is given by

$$\mu(N) = \frac{dE(N)}{dN}, \quad (2)$$

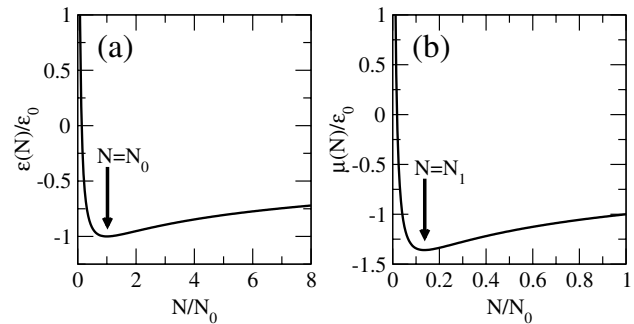


FIG. 1. (a) Energy per atom  $\varepsilon(N)$  and (b) chemical potential  $\mu(N)$  plotted as a function of  $N/N_0$  for  $W = 0$  and  $C_1/C_2 = 3.27$ . Minima in  $\varepsilon(N)$  and  $\mu(N)$  occur at  $N = N_0$  and  $N = N_1 \approx 0.14N_0$ , respectively.

which is displayed in Fig. 1(b) and has a minimum at  $N_1 = N_0/e^2 \approx 0.14N_0$ .

We will describe the evolution of the 2D strained island nanostructure array by a Fokker-Planck equation which is derived as an approximation of the kinetic Becker-Döring model for the aggregation of particles [28]. It is a standard approach used to discuss time-dependent nucleation [29] and is also directly applicable to studying the time evolution of an array of nanoclusters [30]. If  $f(t, N)$  is the island size distribution function such that  $f(t, N)dN$  specifies the number of islands per unit area containing atoms between  $N$  and  $N + dN$  at time  $t$ , then the appropriate Fokker-Planck equation governing the time evolution of the islands is

$$\frac{\partial}{\partial t} f(t, N) = -\frac{\partial}{\partial N} J(t, N), \quad (3)$$

where the flux in the configurational space of island size is

$$J(t, N) = \omega(N) \left[ \frac{\bar{\mu} - \mu(N)}{k_B T} f(t, N) - \frac{\partial}{\partial N} f(t, N) \right]. \quad (4)$$

Here we have considered the standard case where the kinetics are limited by attachment (detachment) processes to (from) the island perimeter [17,18] and the kinetic factor  $\omega(N) = N^{1/2}$  for appropriate scaling of the units of time. The first term in Eq. (4) is conventionally referred to as the drift contribution and is associated with a drift velocity,

$$u(t, N) = \omega(N) \left[ \frac{\bar{\mu} - \mu(N)}{k_B T} \right]. \quad (5)$$

The second term is known as the diffusion contribution. The time-dependent, mean-field chemical potential  $\bar{\mu}$  is determined from the quasi-steady-state requirement that the island flux  $J(t, N)$  integrated over all islands is equal to the deposition flux  $\Phi$ ;

$$\int_0^\infty J(t, N) dN = \Phi. \quad (6)$$

The evolution of  $f(t, N)$  is obtained by solving Eq. (3) numerically, using the methods outlined in [7,31]. The mean-field chemical potential  $\bar{\mu}$  is evaluated after each time increment using Eq. (6).

We first consider a Gaussian 2D island distribution centered on an island size located significantly below the minimum in  $\mu(N)$  at  $N_1$  and employ our model to calculate the initial evolution of the distribution during ripening (zero flux). We measure the temperature  $T$  with respect to the temperature  $\Theta = C_2 \sqrt{N_0}/k_B$  corresponding to the energy of an island containing  $N_0$  atoms of energy per atom  $\varepsilon_0$  [32]. In all calculations we use  $T/\Theta = 10^{-3}$  and  $C_1/C_2 = 3.27$ , giving  $N_0 = 5.1 \times 10^3$ . The evolution shown in Fig. 2(a) is driven by the negative gradient in  $\mu(N)$  and, as such, is similar to conventional capillarity-driven ripening, in which the chemical potential decreases monotonically. Small islands with a chemi-

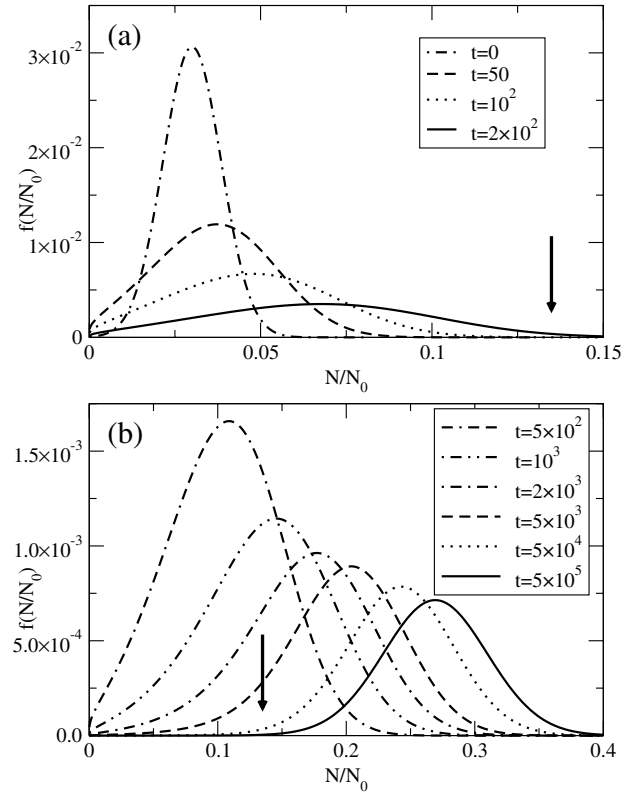


FIG. 2. (a) Early and (b) late evolution of  $f(t, N)$  with time (scaled units) for a Gaussian initial distribution located below  $N_1$ . The solid arrows indicate the chemical potential minimum at  $N_1$ .

cal potential above  $\bar{\mu}$  shrink [according to Eq. (5)] and large islands, with a chemical potential below  $\bar{\mu}$ , grow. The island distribution therefore broadens and evolves to larger volumes as shown.

Figure 2(b) shows the same island distribution evolved to later times. The distribution approaches and, surprisingly, passes slightly above  $N_1$ . By  $t = 5 \times 10^5$ , essentially the whole distribution lies above  $N_1$ . This contrasts with the conventional view that the evolution stops at the chemical potential minimum [16,33]. Note that passing through the minimum is a consequence of the drift term and occurs even with the diffusion term set to zero [34]. Therefore, the minimum in chemical potential does not formally determine an optimum island size, even in the drift dominated regime. Beyond  $N_1$ , the distribution narrows and the subsequent evolution is considerably slower as the drift and diffusion terms compete in Eq. (4). This cancellation of terms produces a metastable state which effectively suppresses the evolution of  $f(t, N)$  on experimentally relevant time scales.

The evolution of an island array located above the minimum in chemical potential exhibits highly unusual behavior. Consider an initial Gaussian distribution centered on an island size much greater than  $N_1$ , as shown in Fig. 3. During ripening, the initial distribution narrows, almost symmetrically, and stabilizes about the mean

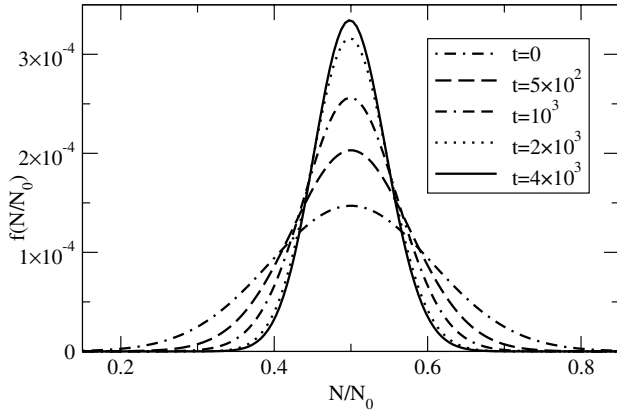


FIG. 3. Evolution of  $f(t, N)$  with time  $t$  (scaled units) for a Gaussian initial distribution located above  $N_1$ . A metastable state is reached by  $t = 4 \times 10^3$ .

island size. This can be simply explained in terms of the mean-field chemical potential  $\bar{\mu}$ . In a drift dominated regime and in the absence of a deposition flux,  $\bar{\mu}$  is a weighted mean of  $\mu(N)$  over  $f(t, N)$  [Eqs. (4) and (6)]. Since  $\mu(N)$  has a positive gradient in this regime, islands will undergo inverse ripening; small islands with a chemical potential below  $\bar{\mu}$  grow and large islands with a chemical potential above  $\bar{\mu}$  shrink. Therefore, the drift term causes the distribution to narrow about the mean island size. However, the diffusion term in Eq. (4) is proportional to  $\partial f(t, N)/\partial N$  and opposes this narrowing, favoring a more disordered system. Eventually, the drift and diffusion terms become very nearly equal in magnitude but opposite in sign, resulting in a long-lived transient state where  $J(t, N) \approx 0$  in Eq. (4) [34]. This dynamic cancellation of competing effects is the origin of the observed metastability in Figs. 2(b) and 3.

A striking feature of the metastable distributions displayed in Figs. 2(b) and 3 is the symmetrical, Gaussian-like profile of the island size distribution function. We can investigate this analytically by noting that the annealed metastable states are associated with a positive gradient in chemical potential for the range  $N_1 < N < N_0$ . To a good approximation, we may represent the variation of  $\mu(N)$  as a straight line over the width of the distribution. Consider, in particular, a metastable state associated with a mean-field chemical potential  $\bar{\mu} = \mu(\bar{N})$  such that the island chemical potential at size  $N$  can be written as  $\mu(N) = (N - \bar{N})d\mu/dN + \mu(\bar{N})$ . Inserting this linear form into Eq. (4) and looking for steady-state solutions satisfying  $J = 0$  yields a metastable Gaussian function centered on  $\bar{N}$ ;

$$f_m(N) = A_m \exp\left[-\frac{d\mu}{dN} \frac{(N - \bar{N})^2}{2k_B T}\right], \quad (7)$$

where  $A_m$  is a constant. We have verified that this analytical form is in excellent agreement with metastable size distribution functions evaluated numerically using

Eqs. (3)–(6) for a range of temperatures [34]. The standard deviation of Eq. (7) is given by  $\sigma = [k_B T / (d\mu/dN)]^{1/2}$  so that narrower distributions would be expected for lower temperatures or steeper gradients in chemical potential. This suggests a means of tuning the distribution width by varying the temperature or the misfit stress (via  $C_2$ ).

It is important to emphasize that approximate solutions of the type given by Eq. (7) are long-lived transient states. They arise due to the effective cancellation of drift and diffusion terms in Eq. (3), which are very nearly equal in magnitude but opposite in sign such that  $J(t, N) \approx 0$  [34]. Over much longer time scales, the system will presumably evolve to the true equilibrium distribution given by the Gibbs-Boltzmann formula  $f_{\text{eq}}(N) = \exp([\bar{\mu}N - E(N)]/k_B T)$ , which is the steady-state solution of Eq. (3) satisfying  $J = 0$ . We note that at equilibrium the entropy contributions associated with finite temperature can lead to a significant broadening of the distribution function and shift the mean island size away from the  $T = 0$  value at  $N_0$  [32].

Metastable states should play a significant role in the coarsening of all surface nanostructures provided that positive gradients in chemical potential exist with respect to island size. Therefore, if material is deposited such that  $\bar{\mu}$  is only slightly enhanced by the deposition flux, the island size distribution will be dominated by the metastable state at that particular coverage. In regions of positive chemical potential gradient, the size distribution can then be tuned to a desired size by depositing material for the required time. With an appropriate value of  $\sigma$  from Eq. (7), this offers the prospect of narrow size distributions which do not significantly broaden with increasing coverage as would be expected in conventional coarsening.

This “close-to-equilibrium” growth procedure is illustrated in Fig. 4 in which we choose a uniform distribution of islands between  $N = 0$  and  $N = 0.07N_0 (< N_1)$  to mimic the early stages of island nucleation [17]. The island array is then evolved in the presence of a small deposition flux which increases the mean-field chemical potential by about 1%. For times smaller than  $t = 10^3$ , the deposition has little effect and the evolution is similar to the zero-deposition case [Fig. 4(a)]. The distribution becomes metastable as it passes above  $N_1$  and further flux causes the Gaussian-like state to drift to higher volumes with only a slight broadening of the profile [Fig. 4(b)].

The unusual characteristic of a coverage dependent mean island size accompanied by a distribution width which is largely independent of coverage, as exhibited in Fig. 4, has recently been experimentally observed for metallic islands [35]. Such islands are thought to possess a minimum in chemical potential with respect to island size (i.e., regions of positive gradient) [33], which, as discussed above, is a necessary condition for the existence of metastable states. The 3D metallic island formation energy is relatively complex compared with 2D

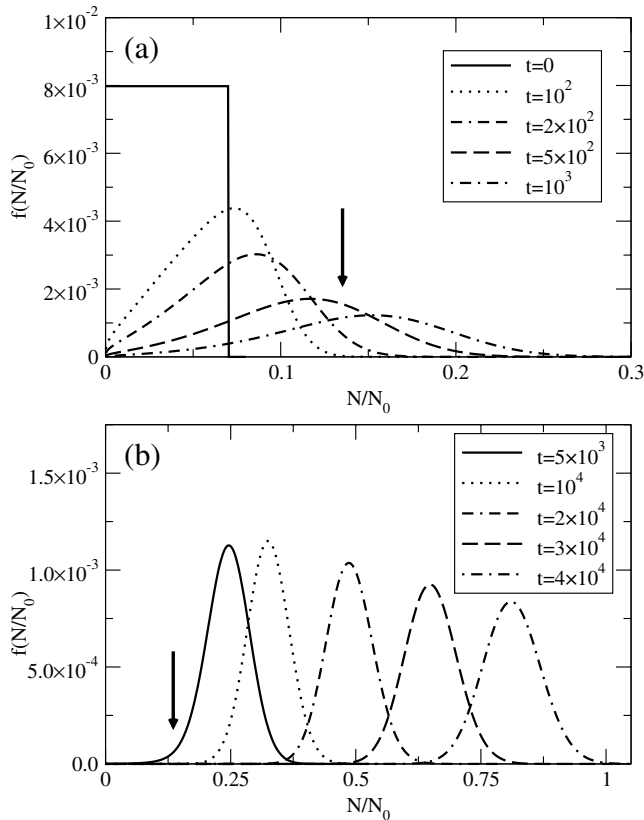


FIG. 4. (a) Early and (b) late evolution of  $f(t, N)$  with time  $t$  (scaled units) for a uniform initial distribution located below  $N_1$  in the presence of a small deposition flux. The solid arrows indicate the chemical potential minimum at  $N_1$ .

islands [33], making a quantitative comparison difficult. However, the general qualitative behavior displayed in Fig. 4 is in excellent agreement with the experimental observations [35,36].

We are grateful to O. Penrose and B.C. Muddle for stimulating discussions. T.P.M. acknowledges a studentship provided by the EPSRC. V.A.S. and D.B. are grateful to the Deutsche Forschungsgemeinschaft (Sfb 296) and the BMBF. V.A.S. acknowledges support from the Russian Foundation for Promotion of Science and from the Russian Foundation for Basic Research.

\*On leave from A.F. Ioffe Physical Technical Institute, St. Petersburg 194021, Russia.

- [1] D.J. Eaglesham and M. Cerullo, Phys. Rev. Lett. **64**, 1943 (1990).
- [2] Y.-W. Mo, D.E. Savage, B.S. Swartzentruber, and M.G. Lagally, Phys. Rev. Lett. **65**, 1020 (1990).
- [3] D. Leonard, K. Pond, and P.M. Petroff, Phys. Rev. B **50**, 11687 (1994).
- [4] J.M. Moison *et al.*, Appl. Phys. Lett. **64**, 196 (1994).
- [5] N.P. Kobayashi, T.R. Ramachandran, P. Chen, and A. Madhukar, Appl. Phys. Lett. **68**, 3299 (1996).

- [6] D. Bimberg, M. Grundmann, and N. Ledentsov, *Quantum Dot Heterostructures* (Wiley, Chichester, 1998).
- [7] H.A. Atwater and C.M. Yang, J. Appl. Phys. **67**, 6202 (1990).
- [8] A.-L. Barabási, Appl. Phys. Lett. **70**, 2565 (1997).
- [9] B.K. Chakraverty, J. Phys. Chem. Solids **28**, 2401 (1967).
- [10] H.T. Dobbs *et al.*, Phys. Rev. Lett. **79**, 897 (1997).
- [11] J. Drucker, Phys. Rev. B **48**, 18203 (1993).
- [12] J.A. Floro *et al.*, Phys. Rev. Lett. **84**, 701 (2000).
- [13] D.E. Jesson, G. Chen, K.M. Chen, and S.J. Pennycook, Phys. Rev. Lett. **80**, 5156 (1998).
- [14] D.E. Jesson, T.P. Munt, V.A. Shchukin, and D. Bimberg, Phys. Rev. B **69**, 041302 (2004).
- [15] I.M. Lifshitz and V.V. Slyozov, J. Phys. Chem. Solids **19**, 35 (1961).
- [16] F. Liu, A.H. Li, and M.G. Lagally, Phys. Rev. Lett. **87**, 126103 (2001).
- [17] F.M. Ross, J. Tersoff, and R.M. Tromp, Phys. Rev. Lett. **80**, 984 (1998).
- [18] W. Theis, N.C. Bartelt, and R.M. Tromp, Phys. Rev. Lett. **75**, 3328 (1995).
- [19] P.W. Voorhees, Annu. Rev. Mater. Sci. **22**, 197 (1992).
- [20] M. Zinke-Allmang, L.C. Feldman, and M.H. Grabow, Surf. Sci. Rep. **16**, 377 (1992).
- [21] V.I. Marchenko, JETP Lett. **33**, 381 (1981).
- [22] D. Vanderbilt, Surf. Sci. **268**, L300 (1992); K.-O. Ng and D. Vanderbilt, Phys. Rev. B **52**, 2177 (1995).
- [23] V.A. Shchukin, N.N. Ledentsov, P.S. Kop'ev, and D. Bimberg, Phys. Rev. Lett. **75**, 2968 (1995).
- [24] I. Daruka and A.-L. Barabási, Phys. Rev. Lett. **79**, 3708 (1997).
- [25] C. Priester and M. Lannoo, Phys. Rev. Lett. **75**, 93 (1995).
- [26] V.A. Shchukin, D. Bimberg, T.P. Munt, and D.E. Jesson, Phys. Rev. Lett. **90**, 076102 (2003).
- [27] R.E. Rudd, G.A.D. Briggs, A.P. Sutton, G. Medeiros-Ribeiro, and R.S. Williams, Phys. Rev. Lett. **90**, 146101 (2003).
- [28] J.J.L. Velázquez, J. Stat. Phys. **92**, 195 (1998).
- [29] J.W. Christian, *The Theory of Transformations in Metals and Alloys, Part I* (Pergamon Press, New York, 2002).
- [30] E.M. Lifshitz and L.P. Pitaevskii, *Physical Kinetics* (Butterworth-Heinemann, Oxford, 1981).
- [31] W.H. Press, S.A. Teukolsky, W.T. Vetterling, and B.P. Flannery, *Numerical Recipes in Fortran 77* (Cambridge University, Cambridge, 1992).
- [32] V.A. Shchukin *et al.*, Phys. Status Solidi (b) **224**, 503 (2001).
- [33] F. Liu, Phys. Rev. Lett. **89**, 246105 (2002).
- [34] D.E. Jesson, T.P. Munt, V.A. Shchukin, and D. Bimberg (to be published).
- [35] Z. Gai *et al.*, Phys. Rev. Lett. **89**, 235502 (2002).
- [36] We note that island coalescence, as considered theoretically in Ref. [14], is most likely contributing to the experimental reduction in island density in Ref. [35]. Although this is not included explicitly in our present analysis it will not alter the major qualitative features of Fig. 4.